EPIGENETICS
2016, VOL. 11, NO. 12, 889–900
http://dx.doi.org/10.1080/15592294.2016.1255385

Taylor & Francis
Taylor & Francis Group

RESEARCH PAPER

PEG3 binds to *H19*-ICR as a transcriptional repressor

An Ye, Hongzhi He, and Joomyeong Kim

Department of Biological Sciences, Louisiana State University, Baton Rouge, LA, USA

ABSTRACT

Paternally expressed gene 3 (*Peg3*) encodes a DNA-binding protein with 12 C2H2 zinc finger motifs. In the current study, we performed ChIP-seq using mouse embryonic fibroblast (MEF) cells. This experiment identified a set of 16 PEG3 genomic targets, the majority of which overlapped with the promoter regions of genes with oocyte expression. These potential downstream genes were upregulated in MEF cells lacking PEG3 protein, suggesting a potential repressor role for PEG3. Our study also identified the imprinting control region (ICR) of *H19* as a genomic target. According to the results, PEG3 binds to a specific sequence motif located between the 3rd and 4th CTCF binding sites of the H19-ICR. PEG3 also binds to the active maternal allele of the H19-ICR. The expression levels of *H19* were upregulated in MEF cells lacking PEG3, and this upregulation was mainly derived from the maternal allele. This suggests that PEG3 may function as a transcriptional repressor for the maternal allele of *H19*. Overall, the current study uncovers a potential functional relationship between *Peg3* and *H19*, and also confirms PEG3 as a transcriptional repressor for the identified downstream genes.

Abbreviations: ICR, Imprinting control region; CTCF, CCCTC-binding factor; MEF, Mouse embryonic fibroblast; ChIP, Chromatin immunoprecipitation; dpc, Days post coitum; FRT, Flippase recognition target

ARTICLE HISTORY
Received 6 September 2016
Revised 6 October 2016
Accepted 24 October 2016

KEYWORDS
CTCF; ChIP-seq; *H19*; imprinting control region; *Peg3*; transcriptional factor

Introduction

Genomic imprinting is an epigenetic process by which one allele of autosomal genes is repressed based on their parental origin.[1] At present, less than 200 genes have been identified as imprinted genes, making up about 1% of the mammalian gene catalog.[2] Imprinted genes are usually clustered in specific chromosomal regions, and these imprinted domains are regulated by *cis* regulatory elements, such as imprinting control regions (ICRs).[3,4] Imprinted genes encode either proteins or noncoding RNA (ncRNA), the majority of which have been shown to play critical roles in controlling embryonic growth and development.[5,6] Some imprinted genes are also known to encode DNA-binding proteins, such as *Zac1* and *Peg3*.[7,8] The DNA-binding protein encoded by *Zac1* binds to the 3′ enhancer of *H19* as a transcriptional activator, suggesting a functional connection between the 2 imprinted genes, paternally expressed *Zac1* and maternally expressed *H19*.[8] Detailed surveys further revealed that many imprinted genes behave coordinately in response to environmental and developmental cues.[8] Thus, the similar expression responses shared among individual imprinted genes have been a basis for the imprinting network model, in which imprinted genes are connected to each other and co-regulated to produce common biological outcomes.[8]

Paternally expressed gene 3 (*Peg3*) is an imprinted gene that encodes a DNA-binding protein.[7] *Peg3* is also a member of an evolutionarily conserved imprinted domain located in human chromosome 19q13.4/proximal mouse chromosome 7.[9,10] This domain is located in the middle of C2H2 Kruppel-type zinc finger gene families.[10] In fact, *Peg3* itself is predicted to encode a protein with 12 C2H2 Kruppel-type zinc fingers.[9,10] Recent studies confirmed that PEG3 indeed binds to a large number of genomic targets as a DNA-binding protein.[7] According to the results, PEG3 functions as a transcriptional repressor for these downstream genes.[7] In particular, PEG3 binds to its adjacent imprinted gene, maternally expressed *Zim1*. Detailed analyses indicated that PEG3 functions as a transcriptional repressor for *Zim1*, possibly through H3K9me3-mediated mechanisms.[11] This possibility has been further supported by the observation that many placenta-specific gene families associated with H3K9me3 modification are de-repressed in mutant embryos lacking PEG3.[12] Although premature at the moment, a series of these recent studies suggested that PEG3 was a transcriptional repressor for its downstream genes through H3K9me3-mediated mechanisms.[11,12]

As an ongoing effort, in the current study we performed a new series of ChIP-seq experiments using mouse embryonic fibroblast (MEF) cells. This series of analyses identified a set of 16 potential downstream genes, and the majority of these genes appear to be expressed in oocytes. Interestingly, one particular target happens to be located within the imprinting control region (ICR) of *H19*. Detailed analyses confirmed the binding of PEG3 to the H19-ICR; expression and *in vitro* analyses further suggest that PEG3 may function as a transcriptional repressor for the maternal allele of the H19-ICR.

CONTACT Joomyeong Kim jkim@lsu.edu Department of Biological Sciences, Louisiana State University, Baton Rouge, LA 70803, USA.
Supplemental data for this article can be accessed on the publisher's website.

Results

Identification of the downstream genes of Peg3 *in MEF cells*

We used a different but improved approach in our PEG3 ChIP-seq experiments compared to the previous study.[7] First, we used chromatin isolated from homogenous populations of MEF cells. Second, we used a mutant model targeting the *Peg3* locus as a negative control.[12] In this knockout (KO) model, transcription of *Peg3* was truncated by 2 poly(A) signals inserted into intron 5 as part of an expression cassette; thus, the PEG3 protein is depleted in these cells (Fig. 1A).[11,12] We first derived a set of MEF cells, wild type (WT) and KO, from 14.5-days post coitum (dpc) embryos that had been prepared through timed mating of male heterozygotes for the KO allele and female littermates. Chromatin prepared from WT and KO MEF cells was individually immunoprecipitated with polyclonal anti-PEG3 antibody.[11] Immunoprecipitated DNA, along with the 2 input DNA, was used for library construction and subsequent sequencing, resulting in 30 to 40 millions reads per sample. These four sets of raw sequence reads have been processed for predicting the potential targets (peaks) of PEG3. This series of bioinformatics processes, described in Material and Methods, derived 2 sets of target regions: one set (56 peaks) from WT and another set (36 peaks) from KO (Supplemental material 1-2). The target regions predicted only from WT, but not from KO, have been further considered as potential target regions for PEG3 (41 peaks). Detailed inspection of these 41 target regions indicated that 31 targets are derived either from the 5′ enhancer, promoter, or 1st intron of 16 individual genes. The remaining 10 targets are derived from the intergenic regions without any obvious gene association. For this study, we further consider a set of 16 genes as potential downstream genes of PEG3 (Table 1). Initial inspection of this set of genes provided the following observations. First, the majority of these genes (13 out of 16) tend to be expressed in mature oocytes, where *Peg3* is repressed by DNA methylation. The expression patterns of potential downstream targets were surveyed through UCSC genome browser (Microarray expression data; http://genome.ucsc.edu/cgi-bin/hgGateway). Second, several genes are closely associated with various cancers, in which *Peg3* is also known to be repressed by DNA methylation.[13,14] These include *Il1r1, Tnik, Pdk2, Rara, Tob2*, and *Mta3*. The expression profiles observed among the downstream genes are inversely correlated with those of *Peg3*. This may be an indication that *Peg3* is a potential repressor for the identified downstream genes. Third, one particular target is localized within the imprinting control region of *H19*, shown as a representative peak in Fig. 1B. This peak is localized between the 3rd and 4th CTCF binding sites of the H19-ICR. The potential binding and subsequent connection of PEG3 to the H19-ICR is very significant given the functional roles played by these 2 imprinted genes; thus, this possibility has been further analyzed in the latter half of the current study. Overall, this series of ChIP-seq experiments identified a set of 16 genes that may be regulated by *Peg3* in MEF cells.

Expression level of downstream genes in MEF cells and neonatal brains

The identified *Peg3* downstream genes were further analyzed as follows. The expression levels of these genes were compared

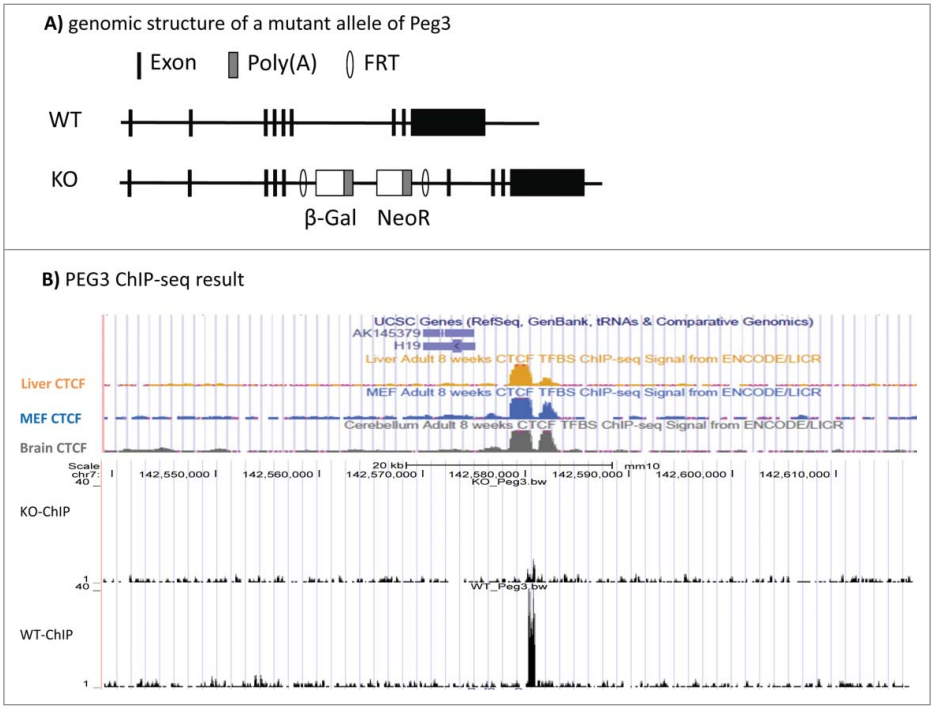

Figure 1. PEG3 ChIP-seq using WT and KO MEF cells. (A) Schematic representation of the genomic structure of the paternally expressed *Peg3*. In the mutant allele, a 7.1-kb cassette containing a promoterless *β*-galactosidase (*β-Gal*) and human *β*-actin promoter-driven neomycin resistant gene (*NeoR*) has been inserted between exon 5 and 6 of *Peg3*. The inserted cassette is flanked by 2 FRT sites (open ovals), thus can be removed through FLP-mediated recombination. (B) CTCF-binding profile and PEG3 ChIP-seq profile on the *H19* locus. The CTCF-binding profiles were derived from MEF cells, brain and liver tissues (upper). PEG3 ChIP-seq profiles were derived from WT and KO MEF cells (lower).

Table 1. Downstream genes of PEG3 in MEF cells (mm9).

Downstream Genes	Chr	Start	End	Log(*P*-value)	Position	Expression in Oocytes
Il1r1	chr1	40332678	40332891	19.98059	1st intron	+++
Prpf18	chr2	4541553	4541865	26.30039	5′ enhancer	++
Prdm11	chr2	92886522	92886836	33.32309	5′ enhancer	+
Tnik	chr3	28161777	28162142	26.96248	5′ enhancer	+
H19	chr7	149766258	149766677	22.19105	5′ enhancer	+
Znrf1	chr8	114060140	114060288	23.08086	promoter	+
Aplp2	chr9	30983874	30984043	18.07835	intron	+
Slc35f2	chr9	53677080	53677370	13.17297	3′ enhancer	++
Pdk2	chr11	94902125	94902816	19.21628	promoter	no
Msl1	chr11	98657458	98658323	26.64127	promoter	++
Rara	chr11	98797334	98797535	28.34715	5′ enhancer	no
Tob2	chr15	81688742	81689010	12.14457	promoter	+++
Dazap2	chr15	100446383	100446839	55.06908	1st intron	++
Ddah2	chr17	35196409	35196881	51.20489	1st intron	no
Mta3	chr17	84105659	84105885	13.16938	1st intron	+++
Msl3	chrX	165112380	165112547	17.96076	promoter	+++

between the WT and KO cells lacking the protein PEG3 by qRT-PCR analyses (Fig. 2). This series of expression analyses used 2 sets of total RNA: the first set was from MEF cells and the second set from neonatal brains. According to the results from MEF cells, the majority of tested genes were upregulated in KO cells, except *Il1r1* and *Slc35f2*. The observed upregulations were statistically significant: 10 genes showed 1.3 to 2.3-fold upregulation while 4 genes displayed more than 3-fold upregulation. Among all the tested genes, *H19* displayed the most dramatic upregulation (6-fold) followed by *Pdk2* (4.3-fold), *Msl1* (3.6-fold), and *Msl3* (3.2-fold). On the other hand, results from neonatal brains displayed overall less dramatic changes. Among 16 tested genes, 6 genes displayed statistically significant changes: 5 genes showed upregulation and 1 downregulation. In particular, the expression level change of *H19* (1.4-fold) was much smaller than the 6-fold upregulation observed in MEF cells. In contrast, the 3 following genes showed more than 2-fold upregulation: *Tnik* (2.3-fold), *Il1r1* (2.9-fold), and *Mta3* (2.7-fold). It is prudent to note that the expression levels of the majority of the genes observed from neonatal brains were much lower than those observed from MEF cells. For instance, the average threshold cycle (Ct) values of the tested genes were around 25 for MEF cells and 30 for neonatal brains, while the Ct values for an internal control *Gapdh* were around 19 to 20 in both cases. This is particularly the case for 2 genes, *Msl1* and *Msl3*, the expression levels of which were almost undetectable in the neonatal brains. Thus, the values for these 2 genes are missing in the neonatal brain set. A similar series of qRT-PCR analyses were also performed using 13-dpc embryos, and the results also indicated that less dramatic changes were observed from embryos of this stage (Supplementary Fig. 1). Overall, this series of analyses demonstrated that the expression levels of the majority of identified downstream genes of *Peg3* were upregulated in cells lacking PEG3, suggesting that PEG3may function as a transcriptional repressor for the identified downstream genes. The observed upregulation was also much more pronounced in MEF cells than in neonatal brains and embryos. We repeated a similar series of expression

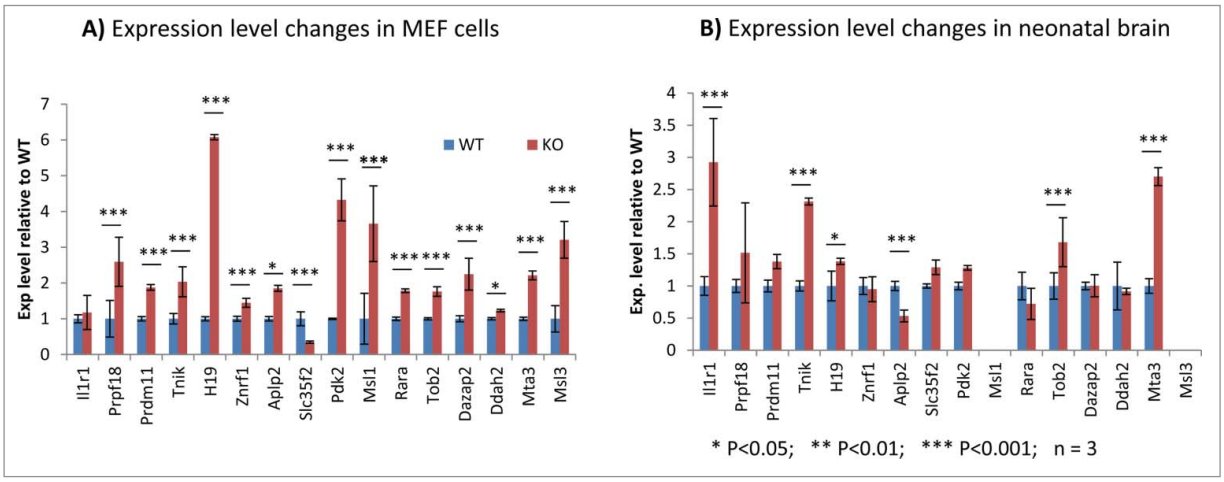

Figure 2. Expression level changes of the identified downstream genes of *Peg3*. A series of qRT-PCR analyses were performed to measure the expression level changes of the potential downstream genes of *Peg3* using the total RNA isolated from the MEF cells (A) and the neonatal brains (B). For each gene, the expression levels were first normalized with an internal control, and the normalized values were subsequently compared between KO and WT samples. The graph summarizes the relative expression levels of each gene with standard deviation, the statistical significance of which was further tested with Mann Whitney U test. This series of expression analyses were also performed using 2 independent sets of MEFs and neonatal brains.

analyses using another set of independent MEFs, neonatal brains, and embryos, and the results were very similar to the patterns described above.

H19 upregulation by PEG3 depletion

The upregulation of *H19* observed in MEF cells and neonatal brains was further characterized (Fig. 3). This upregulation could be either a direct or indirect outcome of PEG3 depletion. Therefore, another series of expression analyses were performed with a set of additional genes that may be associated with the function of the H19-ICR or the transcription of *H19* itself. The list of additional genes includes *Igf2, Igf2r, Ctcf*, and *Zac1*. The transcriptional levels of *Igf2* and *Igf2r* are closely associated with those of *H19*.[15] On the other hand, both *Ctcf* and *Zac1* are known to control the transcription levels of *H19* as activators.[8,16-18] This list also includes 2 unrelated genes, *Yy1* and *p53*, as negative controls. According to the results from MEF cells, the expression levels of 4 genes were upregulated in KO cells: *Ctcf* (1.5-fold), *Zac1* (2.7-fold), *Igf2r* (2-fold), and *Igf2* (7-fold). In contrast, the 2 negative control genes, *Yy1* and *p53*, did not show major differences (greater than 10%) between WT and KO cells, indicating that depletion of PEG3 did not have a global impact on transcription in MEF cells. Interestingly, the 2 known activators for *H19, Ctcf* and *Zac1*, turned out to be upregulated; thus, it is possible that depletion of PEG3 caused upregulation of *H19* through these 2 transcription factors. However, given the expression level changes in these genes, 6-fold change for *H19* vs. 1.5-fold and 2.7-fold change for *Ctcf* and *Zac*, respectively, PEG3 might regulate the expression of *H19* as a trans factor. On the other hand, upregulation of *Igf2* and *Igf2r* was unexpected, since their transcriptional levels, at least for *Igf2*, are usually inversely correlated with those of *H19*.[19] Two independent surveys were also performed using total RNA from neonatal brains and livers. According to the results from the neonatal brain set (Fig. 3B), no major changes between WT and KO were observed, except for the fact that *H19* was still upregulated. In the case of the neonatal liver set, the expression level of *H19* was also upregulated, whereas that of *Igf2* was not affected (Supplementary Fig. 3). Overall, this series of analyses concluded that upregulation of *H19* is likely an outcome of specific changes that happen on the *H19*/*Igf2* locus, but not of global effects that are driven by the depletion of PEG3.

PEG3 binding to the H19-ICR

We also further characterized the potential binding of PEG3 to the H19-ICR using the following approaches. We repeated ChIP experiments using the 2 sets of chromatin prepared from MEF cells and neonatal brains (Fig. 4A). We first tested the feasibility of the ChIP experiments using the known target region phosphoglucomutase 2 like 1 (*Pgm2l1*), as a positive control.[7] As predicted, specific enrichment was detected at the *Pgm2l1* locus in WT cells, but not in the KO cells lacking PEG3. This was also the case for the neonatal brain set, confirming the binding of PEG3 to this locus as well as the specificity of the ChIP experiments. For the actual test on the H19-ICR, we used 2 primer sets: the first set targeting the entire region of the initial peak (H19-ICR, 420 bp in length); the second set targeting the narrow region immediately surrounding the summit of the peak (H19-Peak, 152 bp in length). These primer sets were tested on the 2 sets of ChIP DNA. As shown in Fig. 4A, specific enrichments were indeed observed only from the WT sets, but not from KO sets, confirming the actual binding of PEG3 to the H19-ICR. Quantitative measurement of these enrichments also supported binding of PEG3 to the H19-ICR (Supplementary Fig. 4). The enrichment (or binding) was much more obvious with the second primer set, further suggesting that PEG3

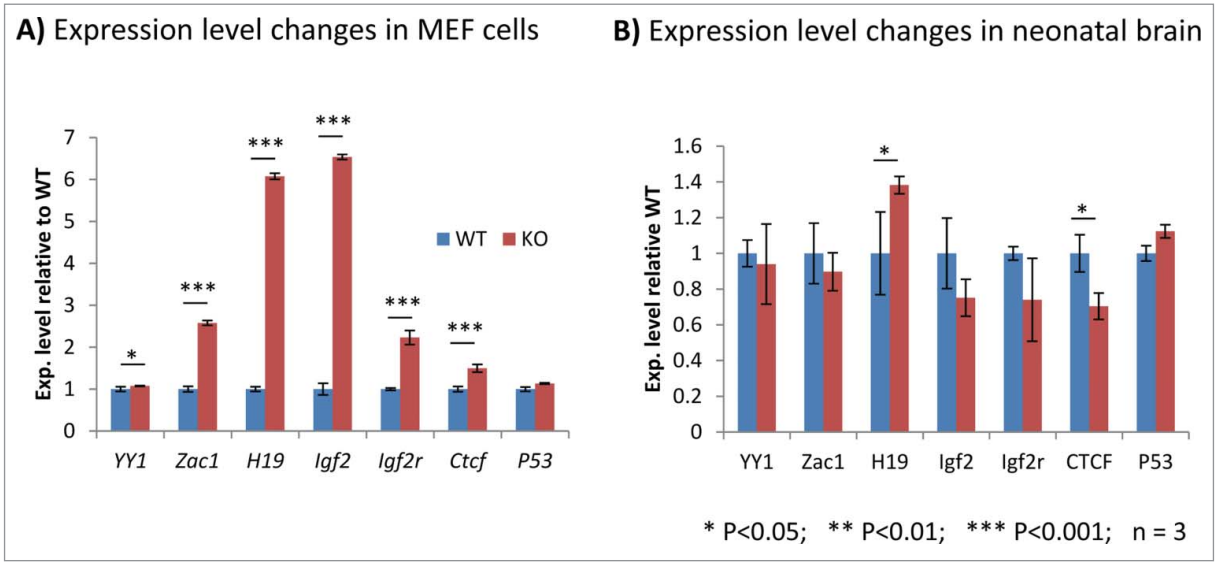

Figure 3. Expression level changes of H19-related genes. A series of qRT-PCR analyses were performed to measure the expression level changes of the genes associated with the H19-ICR or H19 transcription using the total RNA isolated from the MEF cells (A) and the neonatal brains (B). For each gene, the expression levels were first normalized with an internal control, and the normalized values were subsequently compared between KO and WT samples. The graph summarizes the relative expression levels of each gene with standard deviation, the statistical significance of which was further tested with Mann Whitney U test. This series of expression analyses were also performed using 2 independent sets of MEFs and neonatal brains.

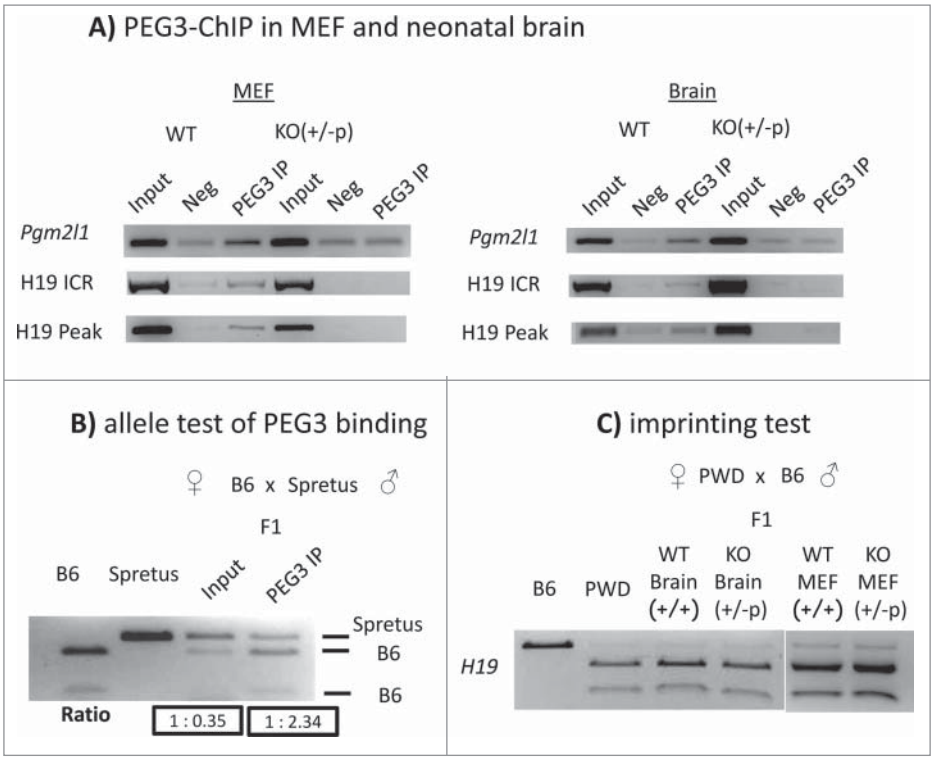

Figure 4. PEG3 binding to the H19-ICR. Individual ChIP experiments were performed to confirm the *in vivo* binding of PEG to the H19-ICR using 2 sets of chromatins prepared from MEF cells and neonatal brains (A). Each set of chromatin was also derived from 2 different samples, representing WT and KO (+/-p) cells. Since *Peg3* is expressed mainly from the paternal allele, the heterozygotes with the paternal transmission are considered to be null. Three individual DNA were derived from each ChIP experiment, and used as templates for PCR survey: Input, Negative control (Neg), and the immunoprecipitated DNA with anti-PEG3 antibody (PEG3 IP). PCR-based surveys tested 3 individual regions: Pgm2l1 as a positive control that has been known to be bound by PEG3, H19 ICR to test the 420-bp-long peak region, and H19 Peak to test the 152-bp-long narrower peak region of the H19-ICR. (B) Allele test of PEG3 binding. Individual ChIP experiments were repeated with the chromatin isolated from the 11.5-dpc F1 hybrid embryos that had been prepared through the crossing between male Spretus and female C57BL/6J (B6). A restriction enzyme digestion (*Acu*I) showed 2 alleles in the Input as well as the immunoprecipitated DNA, but with different ratios between the 2 alleles, which are shown underneath the gel images. (C) Imprinting test of *H19* expression. Total RNA was isolated from 2 sets of the F1 hybrid samples and 2 sets of hybrid MEF cell samples that had been prepared through the crossing between male B6 and female PWD/PhJ. A restriction enzyme digestion (*Bcl*I) showed the 2 parental alleles (lane 1–2), and also the maternal-specific expression in neonatal brains (lane 3–4) and in MEF cells (lane 5–6).

may bind to *cis*-regulatory motifs located within this 152-bp-long genomic interval. As shown for the H19-ICR, an independent ChIP experiment also confirmed the binding of PEG3 to half of the potential targets identified through ChIP-seq (Supplementary Figs. 6 and 7).

Since *H19* is imprinted, we also tested the allele specificity of PEG3 binding to the H19-ICR. For this test, we prepared another set of chromatin isolated from 11-dpc F1 hybrid embryos that had been prepared through the interspecific crossing between male Spretus and female C57BL/6J (B6). As shown in Fig. 4B, restriction enzyme digestion of the input DNA showed 2 parental alleles, although the Spretus allele was over-represented relative to the B6 allele due to the heteroduplex formation between Spretus and B6 strands during PCR and subsequent resistance to the restriction enzyme digestion (1 to 0.35). Nevertheless, digestion of the DNA immunoprecipitated with anti-PEG3 antibody displayed much higher levels of the B6 allele (1 to 2.34), suggesting that PEG3 most likely binds to the maternal allele of the H19-ICR. This further implies that PEG3 may be functionally involved with the maternal allele of the H19-ICR. To further test this possibility, we performed another imprinting test with total RNA isolated from MEF cells and neonatal brains of F1 hybrids that had been prepared through the interspecific crossing between male B6 and female PWD/PhJ. This set of total RNA was first reverse-transcribed and later amplified with a primer set encompassing a sequence polymorphism that can be recognized by the restriction enzyme *Bcl*I (Fig. 4C). The restriction enzyme digestion showed that *H19* was still expressed mainly from the maternal allele in both cells and neonatal brain tissues. This was also the case for the imprinting status of *Igf2*, still showing paternal expression (Supplementary Fig. 2). This indicated that depletion of PEG3 did not cause any change in the imprinting status of *H19*, suggesting no impact on the imprinted paternal allele. Instead, depletion of PEG3 may have an impact on the active maternal allele of the H19-ICR, resulting in the upregulation of *H19* in MEF cells, neonatal brains, and livers. Taken together, this series of analyses suggests that PEG3 most likely binds to the maternal allele of the H19-ICR as a repressor to control the transcriptional levels of *H19*.

PEG3 binding site within the H19-ICR

The predicted binding sites of PEG3 localized within the H19-ICR were further characterized with a series of gel shift assays (Figs. 5 and 6). This series of gel shift assays were performed with several sets of oligonucleotide duplexes. First, a 39-bp-long duplex from the *Pgm2l1* locus was used

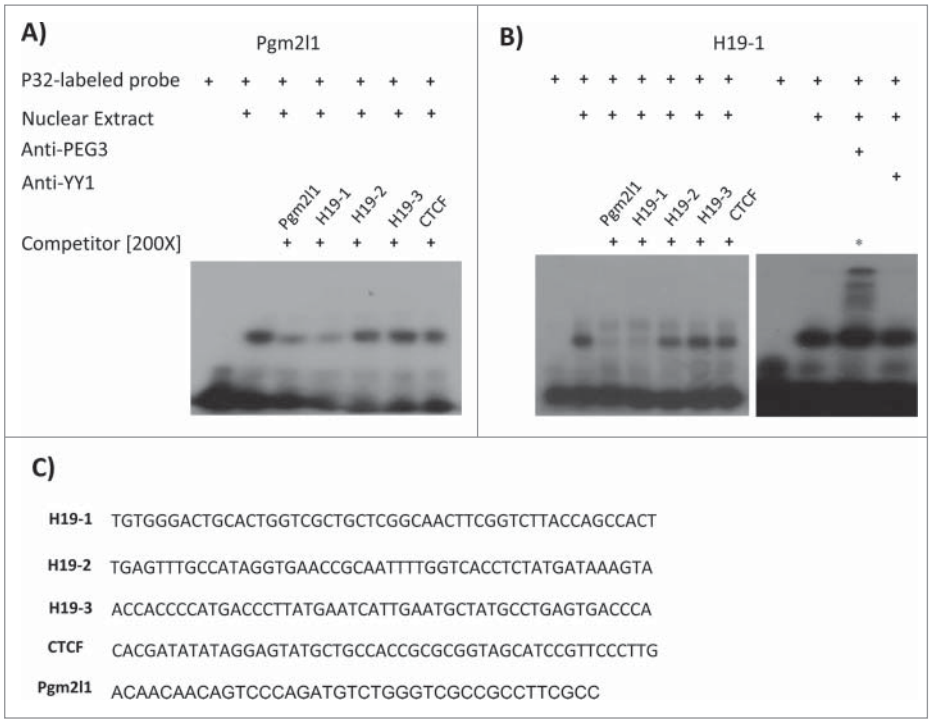

Figure 5. Electromobility shift assay for the DNA-binding sites of PEG3 within the H19-ICR. (A) The 152-bp-long region within the H19-ICR was divided into 3 individual 50-bp-long regions, and used as oligonucleotide duplexes, H19–1, H19–2, H19–3. The 32-bp-long duplex from *Pgm2l1* was used as a P^{32}-radiolabeled probe. The 50-bp-long region surrounding the 3rd CTCF site of the H19-ICR was also included as a control. Excessive amount (200X) of unlabeled Pgm2l1, H19–1, H19–2, H19–3 and CTCF were competed against the radiolabeled H19–1 probe. The H19–1 duplex competed well against the labeled Pgm2l1 probe, indicating that the DNA-binding site for PEG3 is localized within the covered region by H19–1. (B) A reciprocal set of competition assays were also performed using H19–1 as a radiolabeled probe (left). A separate super shift assay was also performed to confirm that the complex binding to H19–1 is indeed the protein PEG3 (right). (C) Shown are the sequences of the duplexes used for the EMSA.

as a positive control, since this locus has been proven to be a target of PEG3.[7] Second, the 152-bp-long H19 Peak region, the smallest target of PEG3 within the H19-ICR (Fig. 4A), was further divided into 3 50-bp-long individual regions, which were subsequently used as a set of 3 testing duplexes, H19–1, −2, and −3. Finally, the 50-bp-long region surrounding the 3rd CTCF site of the H19-ICR was used as a negative control. According to the results, the P^{32}-labeled Pgm2l1 probe was bound by a protein complex known contain PEG3.[7] Among the tested duplexes, H19–1 was shown to compete well against the Pgm2l1 probe, whereas the other 2 duplexes, H19–2 and H19–3, and also the CTCF duplex, did not compete at all. This was further confirmed through a reciprocal set of gel shift assays, in which the H19–1 duplex was used as a P^{32}-labeled probe (Fig. 5B). Consistent with the initial result, the Pgm2l1 duplex was the only duplex that competed well against the H19–1 probe. As expected, the 3 remaining duplexes, H19–2, H19–3 and CTCF, did not compete against the H19–1 probe. Also, a set of super shift assays demonstrated that the protein complex bound by the H19–1 probe is indeed the complex containing PEG3 (Fig. 5B). Taken together, this series of gel shift assays confirmed that the 50-bp-long region covered by the H19–1 duplex most likely contains the binding site for PEG3. Furthermore, this 50-bp-long region may be the only region that is responsible for the binding to PEG3 within the H19-ICR.

The actual binding sites of PEG3 within the H19–1 region were further narrowed down with another set of gel shift assays (Fig. 6). This series of analyses used 2 sets of mutant oligonucleotide duplexes. For the first set of mutant duplexes, the 50-bp-long H19–1 region was again divided into 3 regions, and the sequence of each region was all mutated into As: MuL1, MuL2, and MuL3 (Fig. 6). These three mutant duplexes were tested against the original H19–1 probe. The results indicated that the 2 duplexes, MuL1 and MuL2, did not compete well, suggesting that the region covered by these 2 duplexes likely contains the actual targets of PEG3. Thus, we prepared the second set of mutant duplexes. In this set, the 14-bp-long A stretches of each of the 2 duplexes, MuL1 and MuL2, was further divided into 2 individual stretches of 7-bp-long As: Mu1a, Mu1b, Mu2a, Mu2b. We performed another competition assay with these 4 mutant duplexes. The results indicated that 2 duplexes, Mu1a and Mu2b, did not compete well against the original H19–1 probe, suggesting that these 2 small regions may be the most critical regions for the binding to PEG3. Inspection of these 2 small regions revealed that the 2 contain or overlap with a small motif that resembles part of the known motif of PEG3, GTGG (Fig. 6B).[7] It is also interesting to note that the 450-bp region surrounding 2 CTCF sites also contains 2 potential binding sites for an orphan nuclear receptor family.[20] These two sites, AB-2 and AB-3, are localized just outside of the 2 PEG3 binding sites, thus suggesting that this 450-bp region may be a main regulatory center attracting several transcription factors besides CTCF and PEG3 for the transcription control of *H19* and *Igf2*. Overall, this series of analyses identified 2 7-bp-long small regions within the H19-ICR as potential binding sites for PEG3.

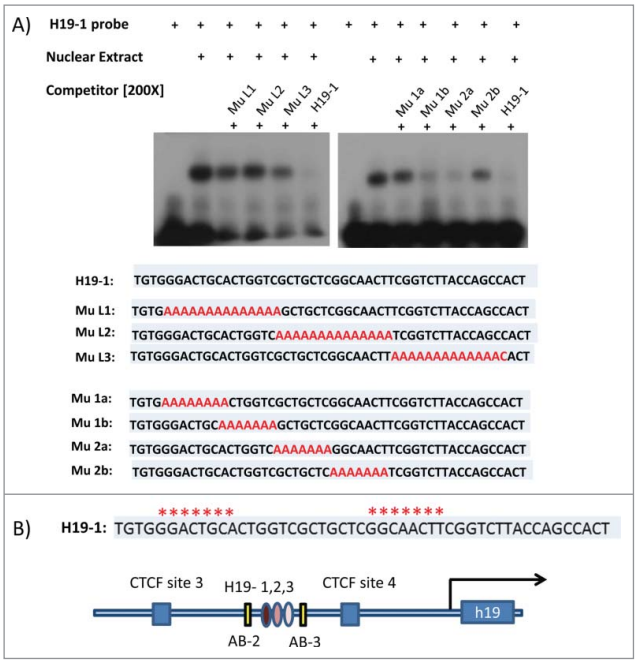

Figure 6. Mutational analyses of the PEG3 binding site of the H19-ICR. The identified 50-bp-long H19–1 region was further analyzed with 2 sets of mutant oligonucleotide duplexes. (A) The 50-bp-long H19–1 was divided into 3 14-bp-long regions, and the bases within each region were all mutated into As. These mutants, MuL1, MuL2, MuL3, were competed against the original H19–1 probe (left). The region covered by MuL1 and MuL2 was further divided into 4 individual 7-bp-long regions, and each region was again mutated with As. These four mutants were competed against the H19–1 probe (right). (B) The results indicated that 2 7-bp-long regions, Mu1a and Mu2b, are the most critical for the binding to PEG3, which are indicated by asterisks (top). The schematic diagram shows part of genomic structure of the H19-ICR with the relative positions of H19–1, H19–2, H19–3, AB-2, AB-3 and 2 CTCF sites (bottom).

PEG3 as a transcriptional repressor for H19

We further tested a potential repressor role of PEG3 in the transcription of *H19* using the following *in vitro* experiments (Fig. 7). As mentioned before, in KO cells transcription of *Peg3* is truncated by the inserted cassette, which is flanked by 2 Flippase Recombination Target (FRT) sites. A vector construct expressing Flippase (FLP) was transiently transfected into the KO cells to remove the cassette, subsequently restoring transcription and translation of *Peg3*. Two additional sets of MEF cells were also transfected as controls: one without vector (Mock) and the other with green florescent protein (GFP) vector. As shown in Fig. 7B, transient expression of FLP indeed removed the inserted cassette based on the detection of a genomic fragment without the inserted cassette. Also, RT-PCR analyses detected transcription of *Peg3* only from KO cells with FLP transfection, but not from the 2 controls, confirming restored expression of *Peg3*. Thus, total RNA was subsequently isolated from the 3 sets of MEF cells for expression analyses of *H19*. According to qRT-PCR results, the expression levels of *H19* in the sample with FLP transfection was indeed downregulated by 20% relative to that from the sample without vector (Mock) (Fig. 7C). This statistically significant downregulation was observed from the sample with FLP, but not from the sample with GFP, thus confirming that the observed downregulation is likely caused by the restored expression of *Peg3*. This further confirmed the repressor role of PEG3 in the regulation of *H19* transcription.

The repressor role of PEG3 was further tested using a series of reporter assays (Fig. 8). A promoterless luciferase vector was used as a basic construct (Basic-Luc), modified first by including the 610-bp-long promoter region of *H19* (H19-Pro), and later by including the 152-bp-long target region of PEG3 (WT-152). Transfection of these constructs into HEK293 cells derived the following outcomes. As expected, the promoter region of *H19* dramatically increased the reporter activity, more than 10-fold. On the other hand, the inclusion of the 152-bp target region of PEG3 resulted in 50% reduction in the promoter activity (Fig. 8A). This suggests that the 152-bp region likely contains repressor elements for the transcription driven by the *H19* promoter. As a second set of assays, the WT-152 construct were co-transfected with varying amounts of the expression vector producing the protein PEG3.[7] The actual expression of the transfected PEG3 vector was further confirmed through Western blotting (Supplementary Fig. 5). As shown in Fig. 8B, transfection with this expression vector at 5X dosage resulted in almost 40% reduction in reporter activity compared to that with no expression vector. This reduction is again consistent with the prediction that PEG3 may function as a repressor for the transcription of *H19*. As a final set of assays, the target region of PEG3 within the WT-152 construct was first mutated, and later co-transfected with the expression vector of PEG3 (Fig. 8C). The results from gel shift assays demonstrated that one 7-bp-long region is critical (Mu2b in Fig. 6). Thus, this region, along with the adjacent 7-bp-long region (Mu2a), was similarly mutated in the WT-152 construct. According to the results, co-transfection of WT-152 with the 5X dosage of the PEG3 expression vector resulted in 30% reduction in the reporter activity. However, the observed reduction disappeared slightly in the Mu2a construct, but completely in the Mu2b construct (Fig. 8C). This indicated that the second 7-bp-long region (Mu2b) is very critical for the repressor role of PEG3. Since this small region is also known to be critical for the binding to PEG3 (Fig. 6), these results strongly support the idea that the repressor role of PEG3 may be mediated through its direct binding to this particular small region of *H19*. Overall, the results described above confirmed that the protein PEG3 likely functions as a repressor for the transcription of *H19*.

Discussion

In the current study, we have identified a set of 16 genes as potential downstream genes of *Peg3* by performing ChIP-seq experiment with MEF cells. The identified genes tend to be expressed in oocytes and also during early embryogenesis. Expression analyses further indicated that the majority of these genes were upregulated in MEF cells lacking the PEG3 protein, thus confirming the repressor role for PEG3. Interestingly, the imprinting control region of the *H19/Igf2* domain turns out to be one of the downstream targets of *Peg3*. The target site is specifically localized between the 3rd and 4th CTCF sites of the H19-ICR. According to the results, PEG3 binds to the active maternal allele of the H19-ICR, and also the depletion of PEG3 resulted in the upregulation of both *H19* and *Igf2* without any

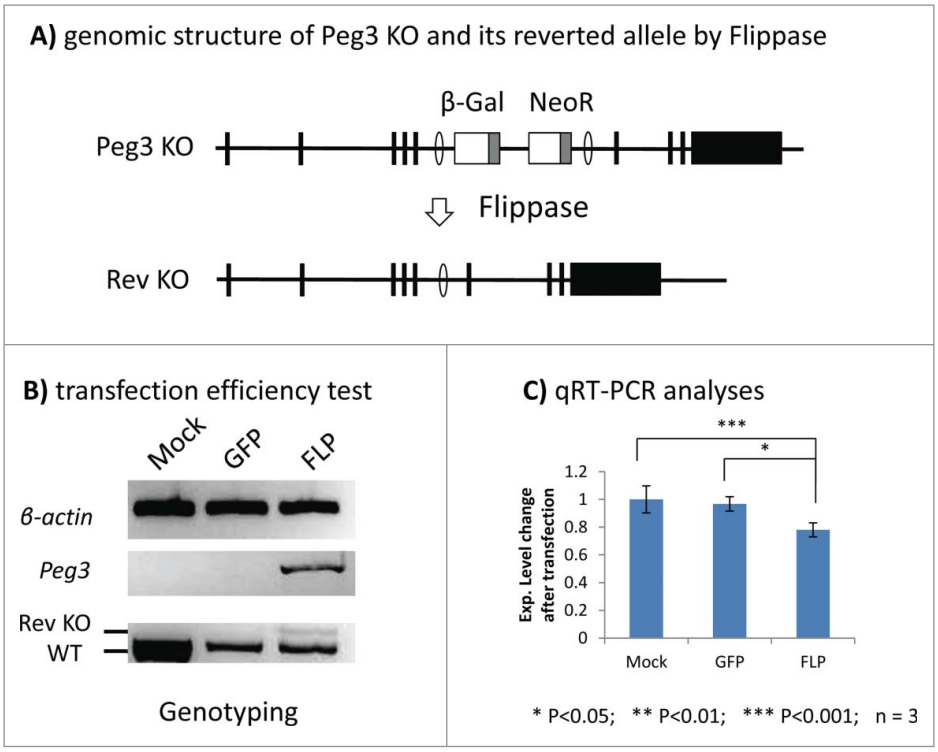

Figure 7. Expression level analyses of *H19* using MEF cells with restored expression of *Peg3*. (A) Genomic structure of the mutant allele of *Peg3* and FLP-mediated recombination scheme to restore the expression of *Peg3*. The inserted cassette is flanked by 2 FRT sites, thus can be removed by Flippase (FLP). (B) Three pools of KO MEF cells were individually transfected with the following constructs: no vector as a mock control (lane 1), a GFP expression vector as a negative control (lane 2), and a FLP expression vector (lane 3). The total RNA isolated from these cells were analyzed with qRT-PCR to measure the expression levels of *β-actin* and *Peg3*. The bottom panel shows genotyping results confirming FLP-mediated recombination of the mutant allele (Rev KO) and endogenous allele (WT) of *Peg3*. (C) The total RNA isolated from the 3 sets of MEF cells were also used for measuring the expression levels of *H19*. The expression level of *H19* was first normalized with an internal control (*Gapdh*), and the normalized values from the 3 sets of MEFs were subsequently compared. The values from the MEF cells transfected with GFP and FLP were divided by the value from a Mock control. Finally, these relative values were presented in the graph with standard deviation, the statistical significance of which was further tested with Mann Whitney U test.

changes in their imprinting status. This confirms a repressor role for PEG3 in the transcriptional regulation of *H19* and *Igf2*. Overall, the current study uncovers a functional connection between the 2 imprinted genes, with the paternally expressed *Peg3* acting as a trans factor controlling the maternally expressed *H19*.

The protein PEG3 appears to control a set of 16 potential downstream genes as a DNA-binding transcription factor (Table 1 and Supplementary Fig. 6). The results from ChIP-seq provide the following insights regarding the function of PEG3. First, the number of potential downstream genes identified from MEF cells is relatively small compared to those from the other known DNA-binding transcription factors, 16 vs. several hundreds.[21] The expression levels of PEG3 are known to be very high in early-stage tissues and neuronal cells.[9] Nevertheless, PEG3 seems to bind to a very small subset of genes in MEF cells. This might be related to the following possibility. PEG3 has been detected not only in the nucleus but also in the cytoplasm, suggesting unknown cytoplasmic functions other than DNA-binding nuclear functions.[22,23] It is possible that only a small fraction of the PEG3 protein functions as a DNA-binding protein, especially in MEF cells. As a consequence, this very limited amount of PEG3 may be available for binding and controlling a small subset of genes. It is, however, also possible that some unknown technical problems involving ChIP and next generation sequencing experiments might have caused this small number of peaks. Second, the identified downstream genes were shown to be all upregulated by the depletion of PEG3 (Figs. 2 and 3). This appears to be consistent with the observations derived from previous studies.[7,11] The two known downstream genes, *Pgm2l1* and another imprinted gene, *Zim1*, were also upregulated in KO cells lacking PEG3. Therefore, it is most likely that PEG3 may also function as a repressor for the newly identified downstream genes. Third, the identified genes seem to share several features, such as expression in oocytes and close association with human cancers. As described earlier, it is interesting to note that the expression level of *Peg3* is very low in both oocytes and some cancers, especially breast and ovarian cancers.[13] This inverse correlation again supports a repressor role of PEG3 for the identified downstream genes. In particular, a subset of these potential downstream genes is highly expressed and also mainly functional during oogenesis and/or early embryogenesis. This subset includes *Msl1* and *Msl3* (Table 1). The expression levels of these genes are very low in the later-stage cells, when *Peg3* is highly expressed. Thus, one of the main functions of *Peg3* might be repressing this set of genes in those somatic cells. Although very speculative at the moment, this might be also one reason why *Peg3* needs to be repressed by DNA methylation during oogenesis. On the other hand, since human *PEG3* has been regarded as a tumor suppressor,[24] the identified downstream genes with cancer connection might provide potential mechanisms by which

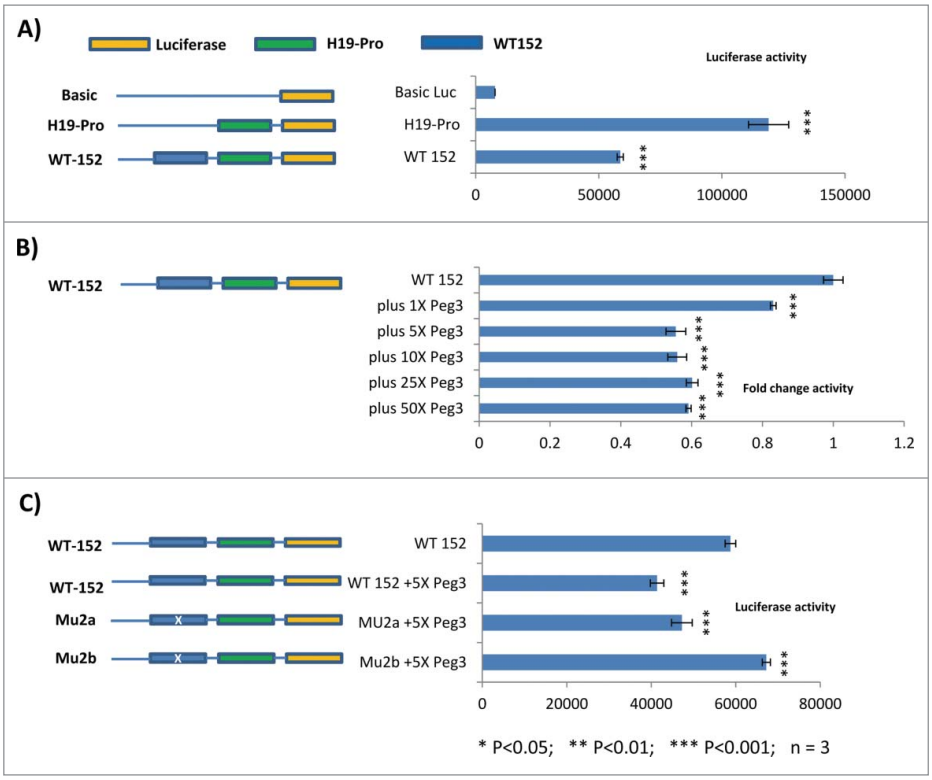

Figure 8. Testing the repressor role of PEG3 through reporter assays. (A) This series of reporter assays used the following 3 constructs. The Basic-Luc construct with a promoterless luciferase reporter was modified first by inserting the 610-bp-long promoter region of *H19* (H19-Pro), and later by inserting the additional 152-bp-long target region of PEG3 (WT-152). The reporter activity from these 3 constructs was summarized and presented as a graph on left. (B) The WT-152 construct was co-transfected with varying amount of the expression vector producing the full-length PEG3 protein. In this series of co-transfection experiments, 10 ng of the expression vector was considered as 1X. The luciferase activity for each sample was first compared to that of the control sample with no expression vector, and this relative value was summarized and presented along with standard deviation on a graph. The statistical significance of the observed change was further tested using Mann Whitney U test. (C) The WT-152 construct was further tested after mutating the potential binding sites of PEG3. The constructs, Mu2a and Mu2b, are identical to WT-152 except that each construct has a 7-bp-long mutation on the critical region for the binding to PEG3. The exact mutation spot for each construct is same as its corresponding duplex mutant used for gel shift assays (Fig. 6).

PEG3 may suppresses tumor formation. For instance, *MTA3* is very closely associated with breast cancer as an oncogene;[25] thus, it would be interesting to further characterize a potential connection between *PEG3* and *MTA3*, specifically to test whether *PEG3* functions as a tumor suppressor by repressing oncogenic *MTA3*. In sum, the protein PEG3 appears to be a transcriptional repressor for a small number of genes that are closely associated with either early developmental processes or human cancers.

One of the unexpected outcomes from the current study was that PEG3 bound to the ICR of the *H19*/*Igf2* domain, specifically to the region between the 3rd and 4th CTCF binding sites (Fig. 1B). This binding by PEG3 also appears to be specific to the maternal allele, which is unmethylated and active (Fig. 4B). Consistent with this, PEG3 binding to DNA is indeed methylation sensitive (Supplementary Fig. 8). The functional outcome of this binding turned out to be repressing the expression of *H19* in MEF cells, 13-dpc embryos, and in the brain and liver of neonates (Figs. 2 and 3, Supplementary Fig. 1 and 3). This has been further followed up with a series of *in vitro* experiments as shown in Figs. 7 and 8, further supporting a repressor role of PEG3 in the expression of *H19*. The observed repressor role of PEG3 is very interesting since this *cis*-regulatory region bound by PEG3 is localized in the middle of the ICR of the *H19*/*Igf2* domain. The ICR of *H19*/*Igf2* has been mainly characterized as a methylation-sensitive insulator region, controlling the allelic expression of both *H19* and *Igf2*. According to the expression analyses, however, the depletion of PEG3 appears to affect mainly the expression levels of *H19*, but not those of *Igf2*: 1.5-fold upregulation of *H19* vs. almost no changes in *Igf2* in the brain and liver of the *Peg3*-KO neonates (Fig. 2B and Supplementary Fig. 3). Although statistically significant, the levels of the observed changes in *H19* expression were relatively small (1.5-fold). This is quite different from the levels of the changes observed from MEF cells, showing 6- to 7-fold upregulation (Figs. 2 and 3). Although the dramatic upregulation in MEF cells is still supportive of a repressor role for PEG3, this observation needs to be interpreted with caution since these tests were performed using an *in vitro* system. In contrast, the much smaller changes observed in *in vivo* tissues might be reflecting the genuine outcome of PEG3 depletion on *H19* expression, and also the possibility much greater changes in *H19* expression might have been lethal during mice embryogenesis. It is also relevant to point out that expression level changes observed in mouse brains might not be as dramatic as in MEFs since those changes are the averaged values of heterogeneous cell populations within brains. Overall, the results described above suggest that the binding of PEG3 to the maternal allele of the ICR is most likely responsible for the transcriptional

regulation of *H19* expression. At the same time, it would be interesting to pursue potential roles for PEG3 in the regulation of *H19* in other tissues, such as testes, where *Peg3* is highly expressed but *H19* is transcriptionally repressed and methylated.

PEG3 depletion seems to have a more complicated and global outcome than expected, according to the results from several series of expression analyses (Figs. 2 and 3 and Supplementary Figs. 1–3). The expression levels of several genes, which are not bound by PEG3, have also been shown to be affected, including *Igf2, Igf2r, Zac1, Peg10, Grb10*, and *Ctcf*. Among these genes, the upregulation of *Igf2* is the most dramatic, with 6-fold upregulation in MEF cells, but no statistically significant changes observed in *in vivo* tissues. The upregulated expression of *Igf2* is still from the paternal allele, which is not bound by PEG3 (Supplementary Fig. 2A). Thus, the upregulation of *Igf2* might be an indirect outcome of the depletion of PEG3. This might also be the case for several other imprinted genes that were also affected, including *Igf2r, Peg10, Zac1*, and *Grb10*. One plausible scenario would be that the observed changes might be reflecting some changes in the proposed imprinted gene network, which might be triggered by the depletion of PEG3.[8] In that regard, it is relevant to point out that *Peg3* is thought to be at the center of this proposed network, meaning that *Peg3* has the most connections with the other imprinted genes.[8] Thus, it is reasonable to predict that the upregulation observed from some of the imprinted genes might be caused by potential disturbance in the imprinted gene network. Overall, depletion of the PEG3 protein has a global impact on the transcription of several other imprinted genes, although it appears to controls only a few imprinted genes, such as *H19*.

Materials and methods

Ethics statement

All the experiments related to mice were performed in accordance with National Institutes of Health guidelines for care and use of animals, and also approved by the Louisiana State University Institutional Animal Care and Use Committee (IACUC), protocol #13–061.

Derivation of MEF cells

Two litters of 14.5-dpc embryos of the C57BL/6J background were harvested through timed mating of the male mice heterozygous for the KO allele with female wild type littermates. The mutant allele of *Peg3* used for the current study has been previously reported and characterized in detail.[12] The head portion and the red tissues were removed from the embryos, and the remaining portions were minced with razor blades. These minced tissues were transferred to a 15-mL conical tubes containing 1 mL trypsin (Invitrogen, Cat. No. 25300062). After 5 min incubation at 37°C, the cells were harvested with centrifugation, and later resuspended in 15 mL media (Life technologies, Cat. No.10566024). Finally, the resuspended cells were plated onto a T-75 flask. The MEF from each embryo was first genotyped using the following primer set: Peg3-for (5′-ATGAGTCTCGATCCCAGGTATGCC-3′) and LoxR (5′-TGAACTGATGGCGAGCTCAGACC-3′). Gender of each MEF was also determined using the following primer set: mSry-F (5′-GTCCCGTGGTGAGAGGCACAAG-3′) and mSry-R (5′-GCAGCTCTACTCCAGTCTTGCC-3′).

ChIP and ChIP-seq analyses

Chromatin was prepared from 2 different types of samples, MEF and neonatal brains, according to the method previously described.[7] In brief, the homogenized samples were first cross-linked with 1% formaldehyde for 20 mins, and then lysed with the buffer containing protease inhibitor cocktail (Millipore, Cat. No. 539131). The released nuclei were fractionated with sonication to derive a pool of DNA fragments sizes ranging from 300 to 500 bp in length. The prepared chromatin was immunoprecipitated with a commercial anti-PEG3 antibody (Abcam, Cat. No. ab99252). The immunoprecipitated DNA was dissolved in 100 μl of TE for PCR analyses. For ChIP-seq analysis, 2 pools of MEF cells (WT and KO) were individually immunoprecipitated with the anti-PEG3 antibody. The two immunoprecipitated DNA along with the 2 corresponding input DNA were used for constructing libraries for ChIP-seq experiments according to the manufacturers' protocol (Illumina FC4014003). The raw sequence reads derived from these 4 libraries, on average 35 millions read per sample, were mapped to the mouse reference genome sequence (mm9) using Bowtie2.[26] The sam files from the mapping were first converted into bed files using Samtools, and later the bed files were used for predicting peaks using MACS2.[27] The final outputs from MACS2 describing ChIP-seq peaks are available (Supplemental material 1–2).

Electromobility shift assay

Electromobility shift assay (EMSA) was performed using a gel shift assay system kit (Promega Cat. No. E3053). This series of assays also used mouse brain nuclear extract (Active Motif Cat. No. 36053) since *Peg3* is highly expressed in the brain tissue.[9,10] The competition assays were performed in the following manner. Briefly, the binding buffer, 2.72 μg mouse brain nuclear extract and unlabeled competitor oligonucleotide duplexes (1.74 pmol, 200X) were first incubated at room temperature 10 mins. Later, 1 μl of P^{32}-labeled duplex probe (1X) was added and incubated at room temperature for additional 20 mins. The reaction mixture was subsequently separated on a 5% TBE gel (Bio-Rad Cat. No. 456–5014), and exposed to film for 2 to 6 hat −80°C. For super shift assays, the initial reaction mixture was incubated along with an antibody, either anti-PEG3 antibody or anti-YY1 antibody (Santa Cruz, Cat No. 1703X), and later incubated with P^{32}-labeled duplex probe.

Transfection experiments

MEF cells were transfected with the following 2 constructs, GFP (pIRES-puro-GFP) and FLP (pIRES-puro-FLP), using the GenJet transfection reagent (Cat. No. SL100489-MEF). Transfection efficiency was also monitored through GFP expression

under a fluorescence microscope at 24-hour post transfection. The transfected cells were harvested at 72-hour post transfection for RNA and DNA isolation. The reverted allele of *Peg3* by FLP was detected through PCR with the following primer set: Flpko-F (5′-CCCTCAGCAGAGCTGTTTCCTGCC-3′) and Flpko-R (5′-AAGCTACCTGGGAAATGAGTGTGG-3′).

RNA isolation and qRT-PCR analyses

Total RNA was isolated from either MEF or the brains of one-day-old neonates using a commercial kit (Trizol, Invitrogen). The total RNA was then reverse-transcribed using the M-MLV kit (Invitrogen), and the subsequent cDNA was used as a template for quantitative PCR. The qRT-PCR analysis was performed with SYBR Select Master Mix (Applied Biosystems, Life Technologies) using the iCycler iQTM multicolor real-time detection system (Bio-Rad). All qRT-PCR reactions were carried out for 40 cycles under standard PCR conditions with internal controls (*Gapdh* and *β-actin*). The results derived from qRT-PCR were further analyzed using the threshold (Ct) value. The ΔCt value was initially calculated by subtracting Ct value of a testing replicate of a given gene from the average Ct value of the internal control (*Gapdh* and *β-actin*). The fold difference for each replicate was then calculated by raising the ΔΔCt value as a power of 2.[28] The average and standard deviation for each sample were then calculated by compiling the normalized values. The information regarding individual primer sequences is also available (Supplemental material 3).

Luciferase reporter assay

This series of reporter assays used the modified version of *β*-geo vector[29] as a control vector monitoring transfection efficiency, and also the modified version of luciferase vector (Promega, PGL3) as a basic construct testing the promoter and the PEG3-bound regions of *H19*. The 610-bp-long promoter region of *H19* was first inserted into the *Not*I site of the promoterless luciferase vector (Basic-Luc). Then, this constructed vector (H19-Pro) was further modified by inserting individually 3 152-bp-long target and its mutated versions (WT-152, Mu2a, Mu2b) into the 5′ region of the 610-bp promoter of *H19*. For luciferase assay, HEK 293 cells were cultured in DMEM plus GlutaMAX medium with 10% fetal bovine serum and 1% antibiotic-antimycotic (GibcoBRL), and plated in 12-well plates for plasmid transfection. The cells on each well were transfected with 4 μl lipofectamine 2000 (Invitrogen) and 1.6 μg of total reporter construct (0.8 μg *β*-geo vector and 0.8 μg luciferase vector) either alone or with the expression vector containing full-length PEG3. For a series of co-transfection experiments, an additional 10 ng of the expression vector of PEG3 was regarded as 1X, 50 ng as 5X, and so forth. Fresh complete media was added 6 hafter transfection, and total cell lysates were harvested in 300 μl of cell lysis buffer 48 hlater according to our previously published protocol.[29] The luciferase assay was performed in triplicate, as previously published.

Disclosure of potential conflicts of interest

No potential conflicts of interest were disclosed.

Acknowledgments

We would like to thank Drs. Suman Lee and Maheshi Dassanayake at LSU and Alvaro Hernandez at University of Illinois for their help in next generation sequencing runs. We also thank Dr. Hana Kim for her help in performing luciferase assays, and also the members of Joo Kim Lab for the detailed suggestions for the manuscript.

References

1 Barlow DP. Genomic imprinting: a mammalian epigenetic discovery model. Annu Rev Genet 2011; 45:379-403; PMID:21942369; http://dx.doi.org/10.1146/annurev-genet-110410-132459
2 Barlow DP, Bartolomei MS. Genomic imprinting in mammals. Cold Spring Harb Perspect Biol 2014; 6(2); http://dx.doi.org/10.1101/cshperspect.a018382
3 Wan LB, Bartolomei MS. Regulation of imprinting in clusters: noncoding RNAs versus insulators. Adv Genet 2008; 61:207-23; PMID:18282507
4 Edwards CA, Ferguson-Smith AC. Mechanisms regulating imprinted genes in clusters. Curr Opin Cell Biol 2007; 19:281-9; http://dx.doi.org/10.1016/j.ceb.2007.04.013
5 Ivanova E, Kelsey G. Imprinted genes and hypothalamic function. J Mol Endocrinol 2011; 47:R67-74; PMID:21798993; http://dx.doi.org/10.1530/JME-11-0065
6 Miyoshi N, Barton SC, Kaneda M, Hajkova P, Surani MA. The continuing quest to comprehend genomic imprinting. Cytogenet Genome Res 2006; 113:6-11; PMID:16575156; http://dx.doi.org/10.1159/000090808
7 Thiaville MM, Huang JM, Kim H, Ekram MB, Roh TY, Kim J. DNA-binding motif and target genes of the imprinted transcription factor PEG3. Gene 2013; 512:314-20; PMID:23078764; http://dx.doi.org/10.1016/j.gene.2012.10.005
8 Varrault A, Gueydan C, Delalbre A, Bellmann A, Houssami S, Aknin C, Severac D, Chotard L, Kahli M, Le Digarcher A, et al. Zac1 regulates an imprinted gene network critically involved in the control of embryonic growth. Dev Cell 2006; 11:711-22; PMID:17084362; http://dx.doi.org/10.1016/j.devcel.2006.09.003
9 Kuroiwa Y, Kaneko-Ishino T, Kagitani F, Kohda T, Li LL, Tada M, Suzuki R, Yokoyama M, Shiroishi T, Wakana S, et al. Peg3 imprinted gene on proximal chromosome 7 encodes for a zinc finger protein. Nat Genet 1996; 12:186-90; PMID:8563758; http://dx.doi.org/10.1038/ng0296-186
10 Kim J, Ashworth L, Branscomb E, Stubbs L. The human homolog of a mouse-imprinted gene, Peg3, maps to a zinc finger gene-rich region of human chromosome 19q13.4. Genome Res 1997; 7:532-40; PMID:9149948
11 Ye A, He H, Kim J. Paternally expressed Peg3 controls maternally expressed Zim1 as a trans factor. PLoS One 2014; 9:e108596; http://dx.doi.org/10.1371/journal.pone.0108596
12 Kim J, Frey WD, He H, Kim H, Ekram MB, Bakshi A, Faisal M, Perera BP, Ye A, Teruyama R. Peg3 mutational effects on reproduction and placenta-specific gene families. PLoS One 2013; 8:e83359; PMID:24391757; http://dx.doi.org/10.1371/journal.pone.0083359
13 Feng W, Marquez RT, Lu Z, Liu J, Lu KH, Issa JP, Fishman DM, Yu Y, Bast RC, Jr. Imprinted tumor suppressor genes ARHI and PEG3 are the most frequently down-regulated in human ovarian cancers by loss of heterozygosity and promoter methylation. Cancer 2008; 112:1489-502; PMID:18286529; http://dx.doi.org/10.1002/cncr.23323
14 Dowdy SC, Gostout BS, Shridhar V, Wu X, Smith DI, Podratz KC, Jiang SW. Biallelic methylation and silencing of paternally expressed gene 3 (PEG3) in gynecologic cancer cell lines. Gynecol Oncol 2005; 99:126-34; PMID:16023706; http://dx.doi.org/10.1016/j.ygyno.2005.05.036
15 Gabory A, Ripoche MA, Le Digarcher A, Watrin F, Ziyyat A, Forne T, Jammes H, Ainscough JF, Surani MA, Journot L, et al. H19 acts as a trans regulator of the imprinted gene network controlling growth in mice. Development 2009; 136:3413-21; PMID:19762426; http://dx.doi.org/10.1242/dev.036061
16 Kurukuti S, Tiwari VK, Tavoosidana G, Pugacheva E, Murrell A, Zhao Z, Lobanenkov V, Reik W, Ohlsson R. CTCF binding at the H19 imprinting control region mediates maternally inherited higher-order

chromatin conformation to restrict enhancer access to Igf2. Proc Natl Acad Sci U S A 2006; 103:10684-9; PMID:16815976; http://dx.doi.org/10.1073/pnas.0600326103
17 Engel N, Thorvaldsen JL, Bartolomei MS. CTCF binding sites promote transcription initiation and prevent DNA methylation on the maternal allele at the imprinted H19/Igf2 locus. Hum Mol Genet 2006; 15:2945-54; PMID:16928784; http://dx.doi.org/10.1093/hmg/ddl237
18 Schoenherr CJ, Levorse JM, Tilghman SM. CTCF maintains differential methylation at the Igf2/H19 locus. Nat Genet 2003; 33:66-9; PMID:12461525; http://dx.doi.org/10.1038/ng1057
19 Thorvaldsen JL, Duran KL, Bartolomei MS. Deletion of the H19 differentially methylated domain results in loss of imprinted expression of H19 and Igf2. Genes Dev 1998; 12:3693-702; PMID:9851976; http://dx.doi.org/10.1101/gad.12.23.3693
20 Bowman AB, Levorse JM, Ingram RS, Tilghman SM. Functional characterization of a testis-specific DNA binding activity at the H19/Igf2 imprinting control region. Mol Cell Biol 2003; 23:8345-51; PMID:14585991; http://dx.doi.org/10.1128/MCB.23.22.8345-8351.2003
21 Kim TH, Abdullaev ZK, Smith AD, Ching KA, Loukinov DI, Green RD, Zhang MQ, Lobanenkov VV, Ren B. Analysis of the vertebrate insulator protein CTCF-binding sites in the human genome. Cell 2007; 128:1231-45; PMID:17382889; http://dx.doi.org/10.1016/j.cell.2006.12.048
22 Relaix F, Wei XJ, Wu X, Sassoon DA. Peg3/Pw1 is an imprinted gene involved in the TNF-NFkappaB signal transduction pathway. Nat Genet 1998; 18:287-91; PMID:9500555; http://dx.doi.org/10.1038/ng0398-287
23 Jiang X, Yu Y, Yang HW, Agar NY, Frado L, Johnson MD. The imprinted gene PEG3 inhibits Wnt signaling and regulates glioma growth. J Biol Chem 2010; 285:8472-80; PMID:20064927; http://dx.doi.org/10.1074/jbc.M109.069450
24 Kim J, Bretz CL, Lee S. Epigenetic instability of imprinted genes in human cancers. Nucleic Acids Res 2015; 43:10689-99; PMID:26338779
25 Zhang H, Stephens LC, Kumar R. Metastasis tumor antigen family proteins during breast cancer progression and metastasis in a reliable mouse model for human breast cancer. Clinical Cancer Research 2006; 12:1479-86; PMID:16533771; http://dx.doi.org/10.1158/1078-0432.CCR-05-1519
26 Langmead B, Trapnell C, Pop M, Salzberg SL. Ultrafast and memory-efficient alignment of short DNA sequences to the human genome. Genome Biol 2009; 10:R25; PMID:19261174; http://dx.doi.org/10.1186/gb-2009-10-3-r25
27 Zhang Y, Liu T, Meyer CA, Eeckhoute J, Johnson DS, Bernstein BE, Nussbaum C, Myers RM, Brown M, Li W, et al. Model-based Analysis of ChIP-Seq (MACS). Genome Biology 2008; 9(9):R137; PMID:18798982
28 Winer J, Jung CK, Shackel I, Williams PM. Development and validation of real-time quantitative reverse transcriptase-polymerase chain reaction for monitoring gene expression in cardiac myocytes in vitro. Anal Biochem 1999; 270:41-9; PMID:10328763; http://dx.doi.org/10.1006/abio.1999.4085
29 Kim JD, Yu S, Kim J. YY1 is autoregulated through its own DNA-binding sites. BMC Mol Biol 2009; 10:85; PMID:19712462; http://dx.doi.org/10.1186/1471-2199-10-85